Computers and Concrete, *Vol. 26, No. 2 (2020) 175-183*
DOI: https://doi.org/10.12989/cac.2020.26.2.175

A model to characterize the effect of particle size of fly ash on the mechanical properties of concrete by the grey multiple linear regression

Yunpeng Cui[1a], Jun Liu*[2], Licheng Wang[1b], Runqing Liu[2c] and Bo Pang[1d]

[1]*Faculty of Infrastructure Engineering, Dalian University of Technology, Dalian, China*
[2]*School of Materials Science and Engineering, Shenyang Ligong University, Shenyang, China*

(*Received February 10, 2020, Revised July 10, 2020, Accepted July 28, 2020*)

Abstract. Fly ash has become an important component of concrete as supplementary cementitious material with the development of concrete technology. To make use of fly ash efficiently, four types of fly ash with particle size distributions that are in conformity with four functions, namely, S.Tsivilis, Andersen, Normal and F distribution, respectively, were prepared. The four particle size distributions as functions of the strength and pore structure of concrete were thereafter constructed and investigated. The results showed that the compressive and flexural strength of concrete with the fly ash that conforming to S.Tsivilis, Normal, F distribution increased by 5-10 MPa and 1-2 MPa, respectively, compared to the reference sample at 28 d. The pore structure of the concrete was improved, in which the total porosity of concrete decreased by 2-5% at 28 d. With regarding to the fly ash with Andersen distribution, it was however not conducive to the strength development of concrete. Regression model based on the grey multiple linear regression theory was proved to be efficient to predict the strength of concrete, according to the characteristic parameters of particle size and pore structure of the fly ash.

Keywords: fly ash; particle size; concrete; grey multiple linear regression

1. Introduction

To date, fly ash has become one of the indispensable materials in cement and concrete due to its unique chemical activity and physical properties, resulting in large volume consumption of fly ash. The price arises gradually (Kumar and Goyal 2019, Khan and Ali 2019, Nguyen *et al*. 2019, Yeh 2008) with the decrease of available fly ash stock. Efficient utilization of fly ash has thus become an urgent problem (Nair and Iyyunni 2013, Bhatt *et al*. 2019, Sata *et al*. 2016). There are two solutions to improve the performances of fly ash. One solution is to apply a certain amount of alkali activator to improve the activity of fly ash. However, the hydration environment and interaction reaction with cement were changed concurrently. Another solution is to change the particle size of fly ash, where the cement can present a better secondary hydration reaction. (Payá *et al*. 1995) studied the strength of cement mortar with five different particle sizes of fly ash (four fly ash prepared with various particle sizes and pristine fly ash) at 28d age. The experimental results showed that the strength of the cement mortar with fly ash (<30% wt) less than 100 μm in size and the cement mortar with pristine fly ash are almost the same as that without fly ash at 28d. However, the strength of the cement mortar with the fly ash more than 50μm in size decreased significantly. Mehta (1985) found that there are an optimal impact on the hydration effect of fly ash with the particle size at about 10 μm. Sugrañez *et al.* (2013) concluded that the early strength of concrete with 0-3 μm particle size fly ash was improved and the strength of concrete at 28d age with 3-25 μm particle size fly ash was improved. The fly ash with single particle size distribution was wasted in the practical application process.

Researchers found that constructing functions for fly ash with different particle size can be used in the whole particle size range (Qiao *et al*. 2016, Judycki 2014). However, the performance of concrete is discrete due to the discontinuity of fly ash particle size. This discrete trend can be mitigated if a mathematical model was built and was able to predict the performance of concrete in the whole particle size range of fly ash. At present, neural network has higher requirements on data samples and prediction stability is widely used. Trend prediction and time series prediction are more sensitive to the external factors. It is easy to emerge large deviation when the external changes are strong (Xu *et al*. 2014, Kongar and Gupta 2019, Micelli and Aiello 2017, Rahimi and Allahyari 2017). More accurate predictions are made according to grey prediction theory with a small amount of data in the insufficient and uncertain information system (Xu *et al*. 2019, Lai *et al*. 2012, Pacheco *et al*. 2020). The grey multiple linear regression method is used to detect and modify the grey prediction model, and the improved grey multiple linear regression combination

*Corresponding author, Professor
E-mail: liujun2699@126.com
[a]Ph.D. Student
E-mail: 232404386@qq.com
[b]Professor
E-mail: wanglich@dlut.edu.cn
[c]Professor
E-mail: 13940195514@163.com
[d]Ph.D. Student
E-mail: pangbo0829@mail.dlut.edu.cn

ISSN: 1598-8198 (Print), 1598-818X (Online)

Table 1 Chemical composition of P▪O 42.5 cement (wt %)

SiO_2	Al_2O_3	Fe_2O_3	CaO	MgO	SO_3	R_2O	Loss of ignition
21.72	5.81	4.33	62.41	1.73	2.56	0.50	1.47

Table 2 Chemical composition of fly ash (wt%)

SiO_2	Al_2O_3	Fe_2O_3	CaO	MgO	Fe_2O_3	SO_3
58.95	26.78	1.53	4.35	2.30	1.53	1.46

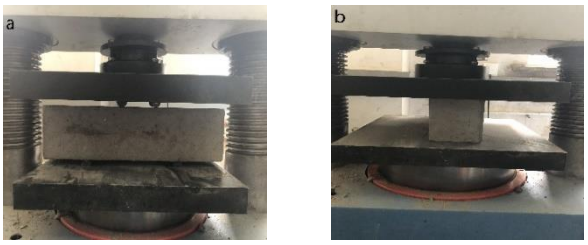

Fig. 1 The measurement of flexural strength and compressive strength (a: flexural strength; b: compressive strength)

model is obtained (Deepak and Davim 2019). The interference of the original data random fluctuation is reduced and the performance prediction is completed combined with multiple factors affecting the order quantity by means of the model (Ma and Liu 2018).

In this work, functions such as close-packing function, activity distribution function and common probability functions are selected. The influence of fly ash with different particle size distribution on the mechanical properties of concrete was studied according to the grey multiple linear regression analysis method. The correlation among fly ash with different particle size distribution, the mechanical properties and pore structure of concrete were analyzed. Then, the mathematical model of fly ash with different particle size distribution areas, the strength and pore structure of concrete were established. The strength of concrete was predicted, from which accuracy and reliability of the prediction were significantly improved.

2. Materials and experiments

CEM 42.5R cement is supplied by Liaoning Shenyang Jidong Cement Co., Ltd. Fly ash (grade II) is supplied by Shenhai thermal power station. The main chemical compositions of raw materials are listed in Table 1 and Table 2. In this experiment, the ratio of cement to sand is 1:3, the ratio of water to cement is 0.42, the content of fly ash is 10 % by the weight of cement, the mix proportions is shown in Table 3. The mix proportion of all experimental groups is the same, the particle size distribution of fly ash is different as following way. Firstly, a certain amount of raw materials was stirring for 1 min. Then, water was added gradually and continued to stir for 3 min. Mixtures were poured into mould with sizes of 100 mm×100 mm×100 mm and 100 mm×100 mm×140 mm for compressive strength and flexural strength tests. Pastes were demolded after 24 h of casting and placed under the condition of air curing

Table 3 Mix proportion of concrete (wt%)

Sample	Water/cement ratio	Cement /sand ratio	Fly Ash (by mass of cement)	Water reducing agent
Control group	0.42	1:3	0	0.3
Experimental group			10	

(temperature of the 20±2°C and humidity of the 95±2%). The compressive strength and flexural strength of concrete are measured be in accordance with Chinese standard (GB/T 50081-2019), “Standard for test methods of concrete physical and mechanical properties”, as shown in Fig. 1. The mercury intrusion porosimeter (MIP, AUTOPORE IV 9500, USA) was used to characterize the pore structure of concrete.

To improve the macro performance of cement-based materials, the micro particles are filled in the pores of cementitious materials according to the close packing theory and particle distribution technology, so as to reduce the initial porosity of cement-based materials (Topçu and Sarıdemir 2008, Chen and Lee 2019). The most typical S.Tsivilis distribution and Anderson distribution are selected, besides, the most common Normal distribution and *F* distribution in engineering mathematics are also selected. The influence of particle size distribution of fly ash on the mechanical properties of concrete was studied, and the particle size distribution of fly ash was optimized.

(a) S.Tsivilis distribution

According to S.Tsivilis, the strength development of cement were affected with the size of 3-30μm particles, and the content should be ≥65%. The content of particles which are less than 3 μm should be ≤10%. Namely

$$Y(30)\text{-}Y(3)\geq 65\% \quad (1)$$

$$Y(3)\leq 10\% \quad (2)$$

Where: $Y(x)$ is the sieving passing rate (%) when the sieve aperture is x μm.

(b) Anderson distribution

According to Andersen, when the particles with continuous distribution are most closely packed, their particle distribution should satisfy the following equation

$$U(D)=100(D/D_l)^n \quad (3)$$

Where: $U(D)$ is the sieving passing rate (%) with the sieve aperture of D; D is the size of the largest particle in the process of sieving (μm); n is the distribution modulus. Among them, when n=1/3, the powder particles appear the largest bulk density and the smallest porosity (Andreasen 1930).

Dinger and funk *et al*. modified the above equation by introducing limited amounts of small particles in the particle distribution. Assumed D=Ds, then $U(D)$=0; while D=Dl, then $U(D)$=1. At this point, the Andreasen equation is as follows

Table 4 Mass percentage of each particle size range of fly ash with S.Tsivilis distribution (wt%)

Particle size range (μm)	Distribution		
	A	B	C
0-3	0	5	10
3-30	100	82.5	65
30-80	0	12.5	25

Note: A:S.TsivilisDistribution (1); B:S.TsivilisDistribution (2); C:S.TsivilisDistribution (3).

$$U(D) = 100\frac{D^n - D_s^n}{D_l^n - D_s^n} \quad (4)$$

Where: D_l is the size of the largest particle when sieving (μm); *Ds* is the size of the smallest particle when sieving (μm). Dinger *et al*. concluded using computer simulation: when n=0.37, the powder particle system appears the maximum packing density and the minimum porosity.

(c) Normal distribution

The Normal distribution of particles is in accordance with the following equation

$$f(x) = \frac{1}{\sqrt{2\pi}\sigma} e^{-\frac{(x-\mu)^2}{2\sigma^2}} \quad (5)$$

Where: σ^2 is the variance of the random variable following the normal distribution; μ is the mean value of the random variable.

(d) F distribution

The *F* distribution of particles is in accordance with the following equation

$$f_{m,n}(x) = \frac{\frac{\Gamma(m+n)}{2}}{\Gamma\left(\frac{m}{2}\right)\Gamma\left(\frac{n}{2}\right)}\left(\frac{m}{n}\right)^{\frac{m}{2}} x^{\frac{m}{2}-1}(1+\frac{m}{n}x)^{-(m+n)/2} \quad (6)$$

Where: m is the first degree of freedom, that is, the number of independent variables; n is the second degree of freedom, that is, the total number of samples.

The fly ash used in this study was prepared according to the following process: firstly, fly ash was mixed with dispersants and then screened by 13 standard sieves with 13 sizes of 3 μm, 5 μm, 8 μm, 10 μm, 15 μm, 20 μm, 26 μm, 30.8 μm, 38.5 μm, 43 μm, 50 μm, 61 μm and 80 μm in turn, where the standard sieves are in conformity with the "Taylar standard sieves", Thereafter, 13 types of fly ash sources were then obtained, which corresponds to particles with 13 sizes in range of 0-3 μm, 3-5 μm, 5-8 μm, 8-10 μm, 10-15 μm, 15-20 μm, 20-26 μm, 26-30.8 μm, 30.8-38.5 μm, 38.5-43 μm, 43-50 μm, 50-61 μm and 61-80 μm, respectively. Secondly, mass percentage of fly ash that falls in the respective 13 size ranges as per the distribution models was calculated. Then, thirteen fly ash samples were obtained according to the calculated mass percentage from the respectively 13 types of fly ash sources. Finally, the obtained thirteen fly ash samples were mixed uniformly and finally the fly ash with required particle sized distribution as per the distribution models (S.Tsivilis distribution, Anderson distribution, Normal distribution and F distribution) was achieved. The quality of each particle size range is shown in Table 4 and Table 5.

Table 5 Mass percentage of each particle size range of fly ash with Andersen distribution, Normal distribution and F distribution (wt%)

Particle size range (μm)	Distribution							
	D	*E*	*F*	*G*	*H*	*I*	*J*	*K*
0-3	33.47	0	16.08	2.27	0	35.21	1.79	1.62
3-5	6.22	8.78	15.51	3.84	0	17.78	8.81	8.49
5-8	6.73	9.67	26.10	11.80	0.16	20.69	25.66	42.91
8-10	3.28	5.22	15.51	12.52	0.44	9.12	18.08	29.78
10-15	7.24	10.66	21.87	38.50	6.07	11.62	29.83	12.83
15-20	5.76	8.59	4.56	24.32	24.17	3.76	11.81	2.96
20-26	5.75	8.68	0.37	6.39	44.92	1.32	4.02	1.41
26-30.8	4.00	6.07	0	0.36	19.36	0.50	0	0
30.8-38.5	5.26	8.59	0	0	4.79	0	0	0
38.5-43	2.94	4.52	0	0	0.09	0	0	0
43-50	4.19	6.49	0	0	0	0	0	0
50-61	5.86	9.12	0	0	0	0	0	0
61-80	8.64	13.61	0	0	0	0	0	0

Note: *D*: Andersen Distribution (n=1/3); *E*: Andersen Distribution (n=0.37); *F*: Normal Distribution (μ=6.5); *G*: Normal Distribution (μ=12.5); *H*: Normal Distribution (μ=22.5); *I*: F Distribution (1); *J*: F Distribution (2); *K*: F Distribution (3).

3. Results and discussion

3.1 Effect of fly ash with different particle size distribution on the mechanical properties of concrete

The compressive strength and flexural strength of concrete at 3d, 7d, 14d and 28d were shown in Figs. 2-5. In the early period (3d), the compressive strength and the flexural strength of *A* are slightly lower than that of the control group, while the compressive strength and the flexural strength of *B* and *C* are higher than that of the control group. The compressive strength and the flexural strength of *D* and E are generally lower than that of the control group. The compressive strength and the flexural strength of fly ash with the Normal distribution are higher than that of the control group. The compressive strength and the flexural strength of fly ash with *F* distribution are higher than that of the control group, and its growth rate is faster. At the age of 7d, the general trend is the same as that of 3d. However, the compressive strength and flexural strength of fly ash with the Normal distribution decreased, the compressive strength of *F* and the flexural strength of *F*, H are lower than that of the control group. At the age of 14d, the compressive strength and the flexural strength of fly ash with *F* distribution is significantly higher than that of the control group. In the later period (28d), the compressive strength of *B* and the flexural strength of *C* concrete increase rapidly, the compressive strength and flexural strength of fly ash with the Normal distribution concrete are substantially lower than that of the control group.

For S.Tsivilis distribution, the compressive strength

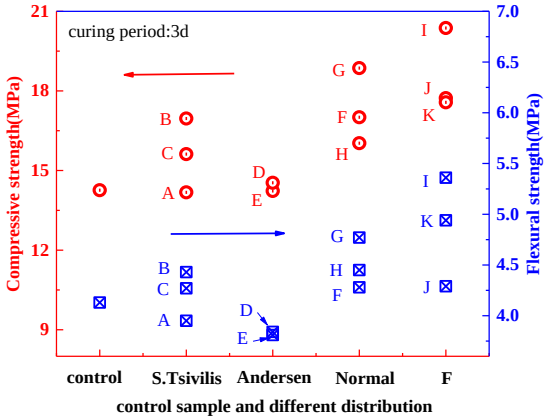

Fig. 2 Compressive strength and flexural strength of concrete in control group and different distribution (curing period: 3d)

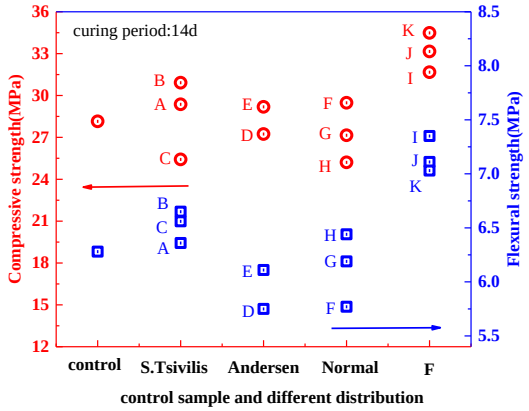

Fig. 4 Compressive strength and flexural strength of concrete in control group and different distribution (curing period: 14d)

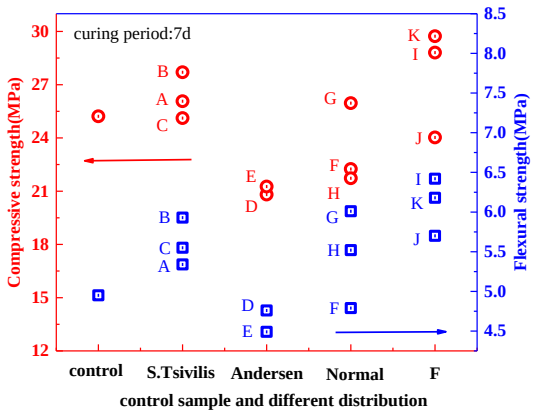

Fig. 3 Compressive strength and flexural strength of concrete in control group and different distribution (curing period: 7d)

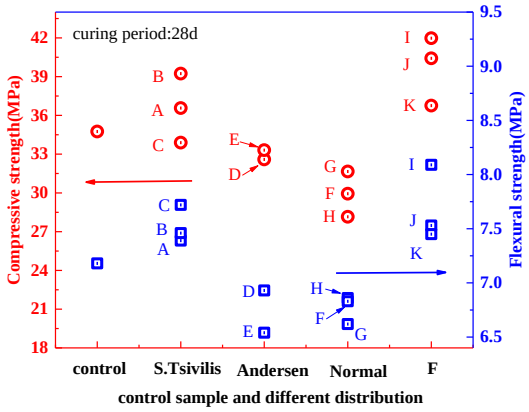

Fig. 5 Compressive strength and flexural strength of concrete in control group and different distribution (curing period: 28d)

(S.Tsivilis (2)) increases by 18.9% and 12.9% at the age of 3 d and 28 d compared with control group, respectively. The flexural strength increases by 7.2% and 3.4% respectively, compared with control group at 3 d and 28 d. Adding fly ash with S.Tsivilis distribution can improve the strength of concrete. At the same time, it shows that the S.Tsivilis distribution is not only suitable for Portland cement, but also for the fly ash with pozzolanic activity. The strength of concrete improved with the change of fly ash size at early and late stage. Ultrafine particles have large specific surface area and high chemical activity, and leads to quick hydration reaction. With the increase of curing age, the contribution of pozzolanic activity of fly ash on strength is increasing, making it higher than that of the control group.

For Anderson distribution, the compressive strength of E concrete increases rapidly at 14 d, the compressive strength increases by 37.3% compared with that of 7 d. The flexural strength of *E* concrete increases rapidly at 14 d, the flexural strength increases by 36.08% compared with that of 7 d. It is not conducive to the strength of concrete that improving the particle size distribution of fly ash to make it the most closely compacted. In other words, it is not conducive to improve the strength of that the fly ash with Andersen distribution concrete. Fly ash with a state of close packing is not play its micro aggregate effect well in the early stage. The total porosity of concrete increases and the number of multiple harmful holes increases. The pozzolanic effect of fly ash plays a major role with the increase of curing age. It will still be affected by its own close packing, and the improvement effect is not ideal.

For Normal distribution, the early of 3 d compressive strength of fly ash with Normal distribution concrete is better, and the compressive strength of *G*, *F* and *H* is 32.25%, 19.28% and 12.41% higher than that of the control group, respectively. The early flexural strength growth rate of *F* and *H* concrete is faster, the flexural strength increases by 24.04% compared with that of 7 d and 25.99% compared with that of 3 d. However, the flexural strength (28d) of H concrete at later stage increases rapidly, the growth value is 38.78%, 18.37% compared with that of 3d and 14d, respectively. When fly ash with the Normal distribution is added, fly ash in the range of 10-15 μm is conducive to improve the early strength of concrete.

For *F* distribution, the compressive strength reaches to 41.98 MPa and 32.55% higher than that of 14 d. the compressive strength (*F* (1)) increases by 42.8% and 20.8% at the age of 3 d and 28 d compared with control group, respectively. The flexural strength increases by 29.7% and

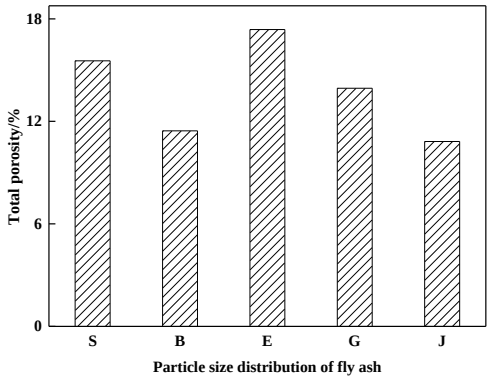

Fig. 6 The calculation results of the total porosity of concrete with different particle size distribution (*S*: control sample; *B*: S.Tsivilis Distribution (2); *E*: Andersen Distribution (n=0.37); *G*: Normal Distribution (μ=12.5); *J*: F Distribution (2))

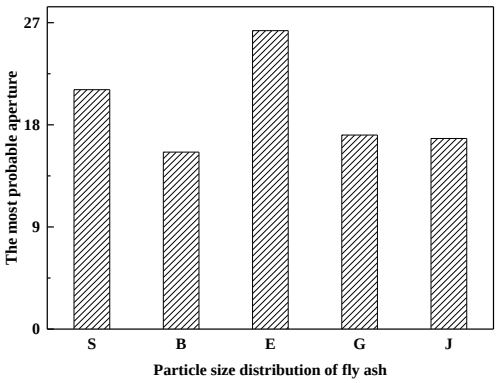

Fig. 7 The calculation results of the most probable pore size of concrete with different particle size distribution (*S*: control sample; *B*: S.Tsivilis Distribution (2); *E*: Andersen Distribution (n=0.37); *G*: Normal Distribution (μ=12.5); *J*: F Distribution (2))

12.6% respectively, compared with control group at 3 d and 28 d. Due to its not in a close accumulation state, the fine particles can participate in the hydration reaction in the later stage, and the pozzolanic activity increases, which has a certain favorable impact on the later compressive strength of concrete. Compared with the other three groups, adding fly ash with *F* distribution is beneficial to improve the compressive strength of concrete. Which shows that the addition of fly ash with *F* distribution is conducive to the improvement of the strength of concrete.

3.2 Effect of fly ash particle size distribution on the pore structure of concrete

The *B*, *E*, *H*, *J* with optimal compressive strength were compared with the control group. Fig. 6 and Fig. 7 are pore structure information of concrete. From the pore structure characteristic parameters of concrete, the development of total porosity and the most probable pore diameter are the same. Except for the *D* and *E* concrete, the total porosity of the rest concrete is reduced. The average pore diameter and the most probable pore diameter are reduced. The structure of *B* and *J* are improved obviously. The porosity are 11.4476% and 10.8231%, respectively. The most probable pore size are 15.6 nm and 16.8 nm, respectively.

It can be seen that there is an obvious regular relationship that the improvement degree of concrete pore structure parameters and fly ash with different particle size distribution. That is, the whole concrete appears close packing state with the addition of fly ash, the better the improvement effect on the pore structure of the concrete is. It is reflected in the distribution of S.Tsivilis (2) and *F* (2) that the appropriate amount of fly ash is increased by 5-15 μm, and the amount of fly ash is reduced by 30-80 μm. The fine particles can fill in the pores of concrete, and the fly ash can play a pozzolanic effect fully at the later stage, the degree of secondary hydration increased, so as to improve the strength. However, the fly ash only present close packing state in the *E* concrete. The packing effect of fly ash and other materials is not well, the pore structure parameters increase and the mechanical properties

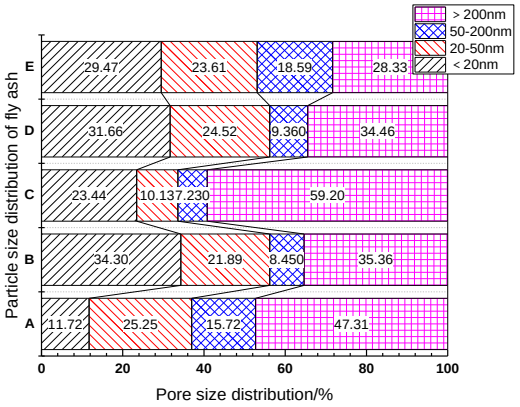

Fig. 8 Pore size distribution of concrete with different particle size distribution

decreases significantly.

As can be seen from Fig. 8, the harmful pores, multiple harmful pores in the vast majority of concrete obviously decreases and the harmless pores increases when different distribution fly ash are added. For example, 15.72% of the harmful pores, 47.31% of the multi harmful pores and 11.72% of the harmless pores are in the benchmark concrete. When *B* and *G* were added into concrete, the harmful pores decreased obviously, which were 8.45% and 9.36% respectively. The multiple harmful pores decreased to 35%, the harmless pores and the less harmful pores increased obviously, which accounted for about 55% of the pore volume. *J* concrete of the multiple harmful pores were the lowest, it was 28.33%; However, *E* concrete under the harmless pore is 23.44%, the multiple harmful pores are 59.20%.

It can be seen that the particle size distribution of fly ash except *E* has obvious effect on improving the pore structure of concrete, which shows a large increment on the strength of concrete. Due to its close packing accumulation state, the packing effect of fly ash and other powder materials is not well. That leads to the highest proportion of multiple damage pores and the strength of concrete greatly reduced. In *F* distribution (2), 5-15 μm fly ash fill in the pores and it

play the role of micro aggregate at the early stage. With the increase of curing age, it is easy to participate in the hydration reaction and make its structure more dense. The multiple harmful pores reduced and the mechanical properties increased.

3.3 The basic principle of grey multiple linear regression analysis

Grey multiple linear regression analysis model (Xie and Yang 2019, Zeng *et al*. 2019, Yu *et al*. 2018) is a multiple linear regression analysis model based on grey system theory. However, it is different from the classical multiple linear regression analysis model. In two aspects: First, the grey multiple linear regression analysis model can improve the problems that the classical analysis model is not reflect the dynamic changes in real time and the system response time is long; Second, the grey multiple linear regression analysis model can effectively reduce the influence of ill-conditioned data on the model when processing data. Due to the data accumulation or subtraction in the classical analysis model, the error of differential equation affects the parameters of estimation. It is more difficult to determine the high-order model and it is usually unstable. In the grey multiple linear regression analysis model, there are N variables in total, which are divided into 1 dependent variable and N-1 independent variable, and there are n time series. Dependent variable prediction value and change trend are predicted mainly using N-1 independent variable in the model.

Assume $Y_1^{(0)}=(y_1^{(0)}(1), y_1^{(0)}(2), \ldots, y_1^{(0)}(n))$ is the sequence of dependent variables, and the sequence of independent variables is as follows:

$$X_1^{(0)}=(x_1^{(0)}(1), x_1^{(0)}(2), \ldots, x_1^{(0)}(n));$$
$$X_2^{(0)}=(x_2^{(0)}(1), x_2^{(0)}(2), \ldots, x_2^{(0)}(n));$$
$$\ldots\ldots \quad \ldots\ldots\ldots$$
$$X_N^{(0)}=(x_N^{(0)}(1), x_N^{(0)}(2), \ldots, x_N^{(0)}(n))$$

The Gray level is weak statistics, which is different from set. That is, the gray level as $g_i=1/\ln(i)$ (i=1, 2, …, n), n is the number of elements to be recognized in the set. It can be seen from the common sense that the gray scale cannot be 1, i is not equal to n, which means things in practice are not fully recognized. According to the definition of gray level, the variable should be multiplied with its own whiteness in different time series. The whiteness is the reciprocal of gray level, which can be set as $w_i=1/g_i=\log 2^{(i)}$, that is, the whiteness of the ith element S_i in S sequence. According to the modeling idea of multiple linear regression analysis, the grey multiple linear regression model satisfies the following matrix equations

$$y_N=\mathrm{BP_N} \tag{7}$$

Among,

$$\mathrm{B}=\begin{bmatrix}\log_2(1)*x_2^{(0)}(1)\log_2(1)*x_3^{(0)}(1)\ldots\log_2(1)*x_N^{(0)}(1)\\ \log_2(2)*x_2^{(0)}(2)\log_2(2)*x_3^{(0)}(2)\ldots\ \log_2(2)*x_N^{(0)}(2)\\ \ldots \quad \ldots \quad \ldots\\ \log_2(n)*x_2^{(0)}(n)\log_2(n)*x_3^{(0)}(n)\ldots\log_2(n)*x_N^{(0)}(n)\end{bmatrix}$$

$$y_N=\begin{bmatrix}[\log_2(1)*x_1^{(0)}(1)\\ \log_2(2)*x_1^{(0)}(2)\\ \ldots\\ \log_2(n)*x_1^{(0)}(n)\end{bmatrix} \qquad P_N=\begin{bmatrix}a\\ b_3\\ b_4\\ \ldots\\ b_N\end{bmatrix}$$

The solution of grey multiple linear regression analysis model is the same as that of classical analysis model, the least square estimation is used to solve the matrix coefficient to get the regression coefficient. According to the above model definition, $y_N=BP_N$

The least square estimation of parameter column PN satisfy the following requirements

$$B^TBP_N=B^Ty_N \tag{8}$$

$$\text{If}(B^TB)^{-1}\text{exist, then}$$
$$P_N=(B^TB)^{-1}B^Ty_N \tag{9}$$

The P_N is solved using MATLAB software, then, substitute it in the prediction expression of grey multiple linear regression analysis model

$$\widehat{y_i}=ax_2^{(0)}(i)+b_3x_3^{(0)}(i)+b_4x_4^{(0)}(i)+\cdots +b_Nx_N^{(0)}(i),(i=1,2,\ldots,n) \tag{10}$$

The value of $\widehat{y_i}$ and $\widehat{y_i}$ are obtained, which is the prediction sequence of dependent variable. Based on the analysis of data, it can be seen that there are a good correlation between the content of fly ash in the four particle size ranges of 3-5 μm, 5-8 μm, 8-10 μm and 10-15 μm and the strength of concrete under the different standard curing condition, which has a significant effect on its improvement. Four kinds different fly ash distribution are selected in the following, the correlation of fly ash particle distribution, strength and pore structure of concrete is studied, the mathematical model is established.

3.4 Mathematical model of fly ash particle size range, flexural strength and pore structure of concrete

Particle size ranges, pore structure and strength of fly ash concrete were shown in Table 6. Among, X is the particle size range (X_1: 3-5 μm, X_2: 5-8 μm, X_3: 8-10 μm, X_4: 10-15 μm); Y is the pore structure parameter (Y_1: porosity, Y_2: average pore size, Y_3, the most probable pore size); Z is the flexural strength of concrete under standard curing; Particle size distribution (S: control group, B: S.Tsivilis distribution (2), E: Anderson distribution (n=0.37), G: Normal distribution (μ=12.5), J: F distribution (2))

Table 6 The values of particle size range, pore structure and strength of fly ash concrete

Variable	Particle size distribution				
	S	*B*	*E*	*G*	*F*
X_1	0.82	0.93	8.78	3.84	8.81
X_2	6.60	7.50	9.67	11.80	25.66
X_3	7.51	8.54	5.22	12.52	18.08
X_4	15.45	17.57	10.66	38.50	29.83
Y_1	15.5456	11.4476	17.3744	13.9371	10.8231
Y_2	26.6	23.8	33.5	26.4	22.9
Y_3	21.1	15.6	26.3	17.1	16.8
Z	6.2	7.3	5.3	7.5	7.1

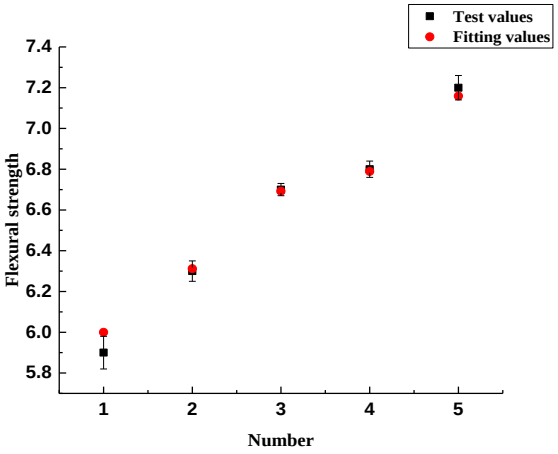

Fig. 9 Relationship between flexural strength of concrete fitting curves and measured values

Under the standard curing condition, there are in good grey multiple linear correlation that the particle size range of fly ash, the characteristic parameters of concrete pore structure and the strength. The fitting function is preliminarily determined as follows

$$Z=AX_1+BX_2+CX_3+DX_4+EY_1+FY_2+GY_3+H \quad (11)$$

Z is flexural strength of concrete; X is particle size range of fly ash; Y is pore structure characteristic parameter of concrete; A-H is corresponding parameter.

The above data are processed using MATLAB software, and the function coefficient parameters are obtained by grey multiple linear regression analysis. The results are shown in formula 12.

$$Z_1=-0.4220X_1+0.0450X_2+0.2995X_3-0.0254X_4 \\ -0.0033Y_1+0.2367Y_2-0.0226Y_3 \quad (12)$$

Finally, the established mathematical model (12) is applied to predict the flexural strength of the above four kinds different fly ash distribution of concrete under standard curing conditions (temperature of the 20±2°C and humidity of the 97±2%) for 7 d curing period. Five groups of concrete were prepared with the numbers of 1-5 respectively. The predicted strength of concrete compared with the actual strength and the results are shown in Fig. 9.

It can be seen from Figure 9 that the predicted flexural strength of concrete is consistent with the actual flexural strength and the similarity is very high. The results show that the mathematical model based on the particle size range of fly ash, pore structure parameters and flexural strength of concrete can be used to predict the flexural strength of concrete under different condition. Meanwhile, the correlation among the particle size range of fly ash, the structural characteristic parameters and the strength of concrete is well, there is a close internal relationship. The validity of the model is further verified by comparison and the predicted strength is basically reasonable and reliable. Therefore, Eq. (12) can be used to characterize the correlation among the particle size range of fly ash, the pore structure characteristic parameters and the flexural strength of concrete.

Table 7 The values of particle size range, pore structure and strength of fly ash concrete

Variable	Particle size distribution				
	S	*B*	*E*	*G*	*F*
X_1	0.82	0.93	8.78	3.84	8.81
X_2	6.60	7.50	9.67	11.80	25.66
X_3	7.51	8.54	5.22	12.52	18.08
X_4	15.45	17.57	10.66	38.50	29.83
Y_1	15.5456	11.4476	17.3744	13.9371	12.8231
Y_2	26.6	23.8	33.5	26.4	22.9
Y_3	21.1	15.6	26.3	17.1	16.8
Z	29.0	32.0	23.4	28.9	25.0

3.5 Mathematical model of fly ash particle size range, flexural strength and pore structure of concrete

Particle size ranges, pore structure and strength of fly ash concrete were shown in Table 7. X is the particle size range (X_1: 3-5 μm, X_2: 5-8 μm, X_3: 8-10 μm, X_4: 10-15 μm); Y is the pore structure parameter (Y_1: porosity, Y_2: average pore size, Y_3: the most probable pore size); Z is the flexural strength of concrete under standard curing; Particle size distribution (S: control group, B: S.Tsivilis distribution (2), E: Anderson distribution (n=0.37), G: Normal distribution (μ=12.5), J: F distribution (2)).

There is a good grey multivariate linear correlation among the particle size range of fly ash, the pore structure parameters of concrete and compressive strength. The fitting function is preliminarily determined as follows

$$Z=AX_1+BX_2+CX_3+DX_4+EY_1+FY_2+GY_3+H \quad (13)$$

Z is flexural strength of concrete; X is particle size range of fly ash; Y is pore structure characteristic parameter of concrete; A-H is corresponding parameter.

The above data are processed using MATLAB software, and the function coefficient parameters are obtained using grey multiple linear regression analysis. The results are shown in formula 14.

$$Z_2=-2.1010X_1+0.0579X_2+1.3563X_3-0.2658X_4 \\ +0.0025Y_1+1.1790Y_2-0.0951Y_3 \quad (14)$$

Finally, the established mathematical model (12) is applied to predict the flexural strength of the above four kinds different fly ash distribution of concrete under standard curing conditions (temperature of the 20±2°C and humidity of the 97±2%) for 7 d curing period. Five groups of concrete were prepared with the numbers of 1-5 respectively. The predicted compressive strength of concrete compared with the actual compressive strength, and the results are shown in Fig. 10.

It can be seen from Fig. 10 that the predicted strength of concrete is consistent with the actual strength, and the similarity is very high. It can be concluded that the mathematical model based on the particle size range of fly ash, pore structure parameters and compressive strength of concrete can be used to predict the compressive strength of concrete under different condition. At the same time, the correlation among the particle size range of fly ash, the pore structure characteristic parameters of concrete and

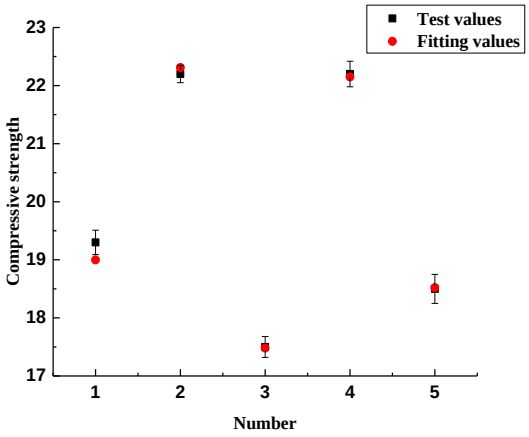

Fig. 10 Relationship between compressive strength of concrete fitting curves and measured values

compressive strength is good and there is a close internal relationship. The validity of the model is further verified by comparison and the predicted compressive strength is basically reasonable and reliable. Therefore, Eq. (14) can be used to characterize the correlation among the particle size range of fly ash, the pore structure characteristic parameters and the compressive strength of concrete under different curing condition.

4. Conclusions

In this paper, the strength properties and pore structure characteristics of concrete mix with fly ash with different particle size distribution function are carried out, and the fitting results are as follows using grey correlation method:

(1) Fly ash conforming to the S.Tsivilis distribution, Normal distribution and *F* distribution can improve the strength of concrete in a certain extent. The compressive and flexural strength of concrete (fly ash with S.Tsivilis, Normal, *F* distribution) increased by 5-10 MPa and 1-2 MPa, respectively, compared to the reference sample at 28 d. Andersen distribution is not conducive to the development of concrete strength.

(2) The S.Tsivilis distribution, Normal distribution and F distribution of fly ash can reduce the porosity, average pore size and the most probable pore size of concrete. The total porosity of concrete decreased by 2-5% at 28 d. Fly ash with Andersen distribution is in close accumulation state and the accumulation with other powder particles is not good, resulting in the highest proportion of multiple damage holes and the strength of concrete is greatly reduced.

(3) The parameters and the prediction fitting equation among the particle size range of fly ash, the pore structure characteristic parameters of concrete and the strength are obtained through the establishment of mathematical model. The fitting effect is good, which shows that the correlation among the particle size range of fly ash, the pore structure characteristic parameters and strength of concrete are good, and there is a close internal relationship.

Acknowledgments

Acknowledgments The authors would like to acknowledge for the financial support by the Key Research and Development Projects of the National 13th Five-Year, (No. 2018YFD1101001)"; National Natural Science Foundation of China, (No. 51972214); Youth Program of National Natural Science Foundation of China, (No. 51902212); Innovation Talents Support Program for Young and Middle-aged People in Shenyang(No. RC190374); Liaoning innovation team support (No. LT2019012); Young Top Talents of Liaoning Province (No. XLYC 1807096).

References

Andreasen, A.H.M. (1930), "Ueber die Beziehung zwischen Kornabstufung und Zwischenraum in Produkten aus losen Körnern (mit einigen Experimenten)", *Kolloid Zeitschrift*, **50**, 217-228. https://doi.org/10.1007/BF01422986.

Bhatt, A., Priyadarshini, S., Acharath Mohanakrishnan, A., Abri, A., Sattler, M. and Techapaphawit, S. (2019), "Physical, chemical, and geotechnical properties of coal fly ash: A global review", *Case Stud. Constr. Mater.*, **11**, e00263. https://doi.org/10.1016/j.cscm.2019.e00263.

Cascardi, A., Micelli, F. and Aiello, M.A. (2017), "An Artificial Neural Networks model for the prediction of the compressive strength of FRP-confined concrete circular columns", *Eng. Struct.*, **140**, 199-208. https://doi.org/10.1016/j.engstruct.2017.02.047.

Chen, H. and Lee, C. (2019), "Electricity consumption prediction for buildings using multiple adaptive network-based fuzzy inference system models and gray relational analysis", *Energy Report.*, **5**, 1509-1524. https://doi.org/10.1016/j.egyr.2019.10.009.

Deepak, D. and Davim, J.P. (2019), "Multi-response optimization of process parameters in AWJ machining of hybrid GFRP composite by grey relational method", *Procedia Manuf.*, **35**, 1211-1221. https://doi.org/10.1016/j.promfg.2019.07.021.

Duman, G.M., Kongar, E. and Gupta, S.M. (2019), "Estimation of electronic waste using optimized multivariate grey models", *Waste Manage.*, **95,** 241-249. https://doi.org/10.1016/j.wasman.2019.06.023.

Judycki, J. (2014), "Influence of low-temperature physical hardening on stiffness and tensile strength of asphalt concrete and stone mastic asphalt", *Constr. Build. Mater.*, **61**, 191-199. https://doi.org/10.1016/j.conbuildmat.2014.03.011.

Kanchana, J., Prasath, V. and Krishnaraj, V. (2019), "Multi response optimization of process parameters using grey relational analysis for milling of hardened Custom 465 steel", *Procedia Manuf.*, **30**, 451-458. https://doi.org/10.1016/j.promfg.2019.02.064.

Khan, M. and Ali, M. (2019), "Improvement in concrete behavior with fly ash, silica-fume and coconut fibres", *Constr. Build. Mater.*, **203**, 174-187. https://doi.org/10.1016/j.conbuildmat.2019.01.103.

Lai, W., Chang, T., Wang, J., Kan, C. and Chen, W. (2012), "An evaluation of Mahalanobis Distance and grey relational analysis for crack pattern in concrete structures", *Comput. Mater. Sci.*, **65**, 115-121. https://doi.org/10.1016/j.commatsci.2012.07.002.

Ma, X. and Liu, Z. (2018), "The kernel-based nonlinear multivariate grey model", *Appl. Math. Model.*, **56**, 217-238. https://doi.org/10.1016/j.apm.2017.12.010.

Mehta, P.K. (1985), "Influence of fly ash characteristics on the strength of portland-fly ash mixtures", *Cement Concrete Res.*, **15**, 669-674. https://doi.org/10.1016/0008-8846(85)90067-5.

Nguyen, T.B.T., Chatchawan, R., Saengsoy, W., Tangtermsirikul,

S. and Sugiyama, T. (2019), "Influences of different types of fly ash and confinement on performances of expansive mortars and concretes", *Constr. Build. Mater.*, **209**, 176-186. https://doi.org/10.1016/j.conbuildmat.2019.03.032.

Nikbin, I.M., Rahimi, S. and Allahyari, H. (2017), "A new empirical formula for prediction of fracture energy of concrete based on the artificial neural network", *Eng. Fract. Mech.*, **186**, 466-482. https://doi.org/10.1016/j.engfracmech.2017.11.010.

Pacheco, J. N., J. de Brito, C. Chastre and L. Evangelista (2020), "Uncertainty of shear resistance models: Influence of recycled concrete aggregate on beams with and without shear reinforcement", *Eng. Struct.*, **204**, 109905. https://doi.org/10.1016/j.engstruct.2019.109905.

Payá, J., Monzó, J., Peris-Mora, E., Borrachero, M.V., Tercero, R. and Pinillos, C. (1995), "Early-strength development of portland cement mortars containing air classified fly ashes", *Cement Concrete Res.*, **25**, 449-456. https://doi.org/10.1016/0008-8846(95)00031-3.

Qiao, Y., Wang, H., Cai, L., Zhang, W. and Yang, B. (2016), "Influence of low temperature on dynamic behavior of concrete", *Constr. Build. Mater.*, **115**, 214-220. https://doi.org/10.1016/j.conbuildmat.2016.04.046.

Sata, V., Ngohpok, C. and Chindaprasirt, P. (2016), "Properties of pervious concrete containing high-calcium fly ash", *Comput. Concrete*, **17**, 337-351. https://doi.org/10.12989/cac.2016.17.3.337.

Singh, N., Kumar, P. and Goyal, P. (2019), "Reviewing the behaviour of high volume fly ash based self compacting concrete", *J. Build. Eng.*, **26**, 100882. https://doi.org/10.1016/j.jobe.2019.100882.

Sugrañez, R., Álvarez, J.I., Cruz-Yusta, M., Mármol, I., Morales, J. and Sánchez, L. (2013), "Controlling microstructure in cement based mortars by adjusting the particle size distribution of the raw materials", *Constr. Build. Mater.*, **41**, 139-145. https://doi.org/10.1016/j.conbuildmat.2012.11.090.

Topçu, B. and Sarıdemir, M. (2008), "Prediction of mechanical properties of recycled aggregate concretes containing silica fume using artificial neural networks and fuzzy logic", *Comput. Mater. Sci.*, **42**, 74-82. https://doi.org/10.1016/j.commatsci.2007.06.011.

Trivedi, J.S., Nair, S. and Iyyunni, C. (2013), "Optimum utilization of fly ash for stabilization of sub-grade soil using genetic algorithm", *Procedia Eng.*, **51**, 250-258. https://doi.org/10.1016/j.proeng.2013.01.034.

Wei, B., Xie, N. and Yang, Y. (2019), "Data-based structure selection for unified discrete grey prediction model", *Exp. Syst. Appl.*, **136**, 264-275. https://doi.org/10.1016/j.eswa.2019.06.053.

Xu, J., Zhao, X., Yu, Y., Xie, T., Yang, G. and Xue, J. (2019), "Parametric sensitivity analysis and modelling of mechanical properties of normal- and high-strength recycled aggregate concrete using grey theory, multiple nonlinear regression and artificial neural networks", *Constr. Build. Mater.*, **211**, 479-491. https://doi.org/10.1016/j.conbuildmat.2019.03.234.

Xu, Q., Shen, Q., Guo, X., Wang, W., Jin, P. and Gong, D. (2014), "Study on the lifetime prediction and evaluation of metering assets based on the multivariate linear regression analysis", *Elec. Measure. Instrum.*, **51**, 17-21.

Yeh, I. (2008), "Modeling slump of concrete with fly ash and superplasticizer", *Comput. Concrete*, **5**, 559-572. https://doi.org/10.12989/cac.2008.5.6.559.

Yu, J., Yoo, J., Jang, J., Park, J.H. and Kim, S. (2018), "A novel hybrid of auto-associative kernel regression and dynamic independent component analysis for fault detection in nonlinear multimode processes", *J. Process Control*, **68**, 129-144. https://doi.org/10.1016/j.jprocont.2018.05.004.

Zeng, X., Shu, L., Yan, S., Shi, Y. and He, F. (2019), "A novel multivariate grey model for forecasting the sequence of ternary interval numbers", *Appl. Math. Model.*, **69**, 273-286. https://doi.org/10.1016/j.apm.2018.12.020.

CC